IEEE Access
Multidisciplinary ⋮ Rapid Review ⋮ Open Access Journal

Received January 4, 2020, accepted January 26, 2020, date of publication February 3, 2020, date of current version February 12, 2020.

Digital Object Identifier 10.1109/ACCESS.2020.2971269

Progressive RSS Data Augmenter with Conditional Adversarial Networks

LIANGFENG CHEN[1], SHUTAO ZHANG[1,2], HAIBO TAN[1], AND BO LV[1]
[1]Hefei Institute of Physical Science, Chinese Academy Sciences, Hefei 230031, China
[2]University of Science and Technology of China, Hefei 230026, China

Corresponding author: Liangfeng Chen (quinear@hfcas.ac.cn)

This work was supported by the Project Intelligence Service Platform for Medium, Small and Micro-Enterprises Based on Big Data funded by Anhui Major Science and Technology Projects under Grant 711245801052.

ABSTRACT Accuracies of most fingerprinting approaches for WiFi-based indoor localization applications are affected by the qualities of fingerprint databases, which are time-consuming and labor-intensive. Recently, many methods have been proposed to reduce the localization accuracy reliance on the qualities of the established fingerprint databases. However, studies on establishing fingerprint databases are relatively rare under the condition of sparse reference points. In this paper, we propose a novel data augmenter based on the adversarial networks to build fingerprint databases with sparse reference points. Additionally, two conditions of these networks are designed to generate data effectively and stably, which are 0-1 sketch and Gaussian sketch. Based on the networks, we design two augmenters with different cyclic training strategies to evaluate the augmenting effects comparatively. Meanwhile, five quantitative evaluation metrics of the augmenters are proposed from two perspectives of the artificial experiences and the data features, and some of them are also used as the gradient penalties for generators. Finally, experiments corresponding to these metrics and localization accuracies demonstrate that the data augmenter with the 0-1 sketch adversarial network is more efficient, effective and stable totally.

INDEX TERMS CGAN, sketch, quantitative evaluation metrics, RSS.

I. INTRODUCTION

The localization awareness is a trend for the hyper-connected society to grow rapidly. Tough outdoor localization-based service (LBS) benefits from the Global Positioning System (GPS) [1], [2], robust LBS for indoor applications is still an open problem [3], [4].

In the past decades, various indoor localization techniques have been proposed, such as infrared equipment localization [5], RFID localization [6], [7], sound localization [8], vision localization [9], Bluetooth localization [10], ultrasonic localization and so on, and WiFi-based localization attracts great attention [11]–[14] since its most applications are realized with the received signal strength (RSS) measured by usual commercial wireless devices without any additional hardware. Among those WiFi-based methods, fingerprinting approaches are remarkable over other methods due to the no need of access points' (APs) localizations, no line of sight (LOS) requirements, and superior localization accuracies [15].

The associate editor coordinating the review of this manuscript and approving it for publication was Qichun Zhang.

The fingerprinting localization usually consists of two phases: the offline phase and the online phase [16]–[18]. In the offline phase, a fingerprint database is constructed with RSS heard from APs in an indoor area, while signal receivers are at the centers of the predefined grids (each grid center is defined as a reference point (RP)). In the online phase, the observed RSS determines the specific localization of a receiver according by a radio fingerprint mapping function. Obviously, the fingerprinting localization accuracy is mainly influenced by two aspects, including the establishment/maintenance of RPs' fingerprint database and the fingerprint matching method.

Many fingerprint matching algorithms have been proposed to improve localization accuracies in recent literatures [19], [20], such as: probabilistic methods [21], [22], k-nearest neighbors (KNN) [23], [24], support vector machine (SVM) [25], [26], artificial neural networks (ANN) [27]–[29], and so on.

ANN has been exhibited into the indoor LBS over a decade ago [30] but has not been widely adopted until recent years due to the outstanding success of the deep learning. Through deep neural networks [31]–[37], more features of the

original localization information are learned efficiently over the conventional methods. In UJIIndoorLoc datasets [38], deep neural networks (DNN) and autoencoders have been proven to be effective in performance improvement. Reference [34] has also proposed an autoencoder with deep extreme learning machine mechanism to locate mobile phones. References [36], [37] have proposed deep convolutional neural networks for indoor localization. In [39] and [40], a feed-forward neural network has been adopted to detect the building, floor and location based on RSS signals. In addition, there are some studies [41]–[44] that convert the 1-D time-series raw signal data into equivalent images and obtain good performance.

In fact, most fingerprinting approaches' accuracies are affected by the qualities of fingerprint databases. Usually, the more RPs preset, the more accurate position results achieve. However, extensive site survey for the fingerprint database is time-consuming and labor-intensive. Especially, once the position environment changes, fingerprint databases and parameters of the position models need to be re-trained to maintain the accuracy [45]. Therefore, many algorithms have been proposed to achieve a given localization accuracy under the sparse RPs condition [18], [46], [47], [48].

Reference [49] provides a calibration zero-effort system based on the crowdsourcing training data and achieves the target tracking with mobile phones. Reference [50] leverages a more stable RSS gradient to avoid the laborious of fingerprint map calibration. Reference [51] proposes a non-intrusive online radio map construction method, where APs are served as online reference points, and achieves the calibration-free indoor localization. In [52], a localization method is proposed to adopt assistant nodes with similar RSS sequences as auxiliary nodes to implement the accurate position. In [53]–[55], fingerprints can be constructed based on the Voronoi diagram according to the signal propagation model [56] and the signal attenuation parameter [57]. Reference [58] applies the surface fitting technique to construct RSS spatial distribution functions. Reference [59] proposes a fingerprint interpolation algorithm to construct its device-specific fingerprints. Reference [60] proposes the RMapTAFA scheme to construct a radio map to improve localization performance of both pedestrian trajectory tracking and stationary point positioning. These methods could decrease the reliance on the accuracies of the established fingerprint databases. However, studies on the fingerprint database under the condition of sparse RPs are relatively rare.

Compared to the existing works, the main contributions of this paper are as follows.

1) A novel type of data augmenters based on conditional generative adversarial networks (GANs) is proposed to generate data from low-level to high-level resolution. Meanwhile, augmenters with different cyclical strategies and conditional sketches are analyzed to offer choices.

2) Two sketches (0-1 sketch and Gaussian sketch) with different priori knowledge are designed as the conditions of GAN. Sketches make adversarial networks learn data features more rapidly and stably. Meanwhile, different sketch elements can be constructed by artificial experiences to adapt varying scenes, such as: LOS/not LOS, heterogenous network and so on.

3) Five quantitative evaluation metrics of GAN are proposed in WiFi-based localization area firstly, and some of them are also used as the gradient penalties for generators.

The rest of this paper is organized as follows. Section II exhibits the data augmenter, including architecture, objective function, sketches and training methods. Some quantitative evaluation metrics of the data augmenter are proposed in Section III. Experiments are given in Section IV to illustrate performances of augmenters. Finally, some conclusions and future works are given in Section V.

II. DATA AUGMENTER BASED ON GAN

To achieve a specific localization accuracy with few or limited RPs by the same mapping function (e.g. KNN), many fake data of virtual RPs are generated by a trained generator G of a conditional adversarial network in this paper, and these data can mix the spurious with the genuine.

The generating progress is also divided into two phases: the training phase of GAN and the generating data phase. In the training phase, random noise is the generator's input, RSS fingerprint data is the real sample and as the discriminator's input, and two sketches with different priori knowledge are the conditions of the generator and the discriminator simultaneously. One manner trained with real RPs only once is defined as Algorithm 1, and the other which is cyclically trained with real and virtual RPs is Algorithm 2. In the generating phase, the trained generators with sketches are used to augment data.

A. PRELIMINARY OF DATA SAMPLES

Firstly, the fingerprint database, which is consisted of RSSs and their corresponding information, such as preset RPs' coordinates, sensor devices, LOS/NLOS, collecting time, etc., is established in order sequence vectors from different APs in a specific indoor environment, and its corresponding variables are defined in Table 1.

Secondly, RSS values in the database need to be normalized by (1) to train GAN.

$$\bar{R}_{C_i}^{k,j} = \begin{cases} \dfrac{R_{max} - R_{C_i}^{k,j}}{R_{max} - R_{min}}, & R_{C_i}^{k,j} < c \\ 1, & R_{C_i}^{k,j} = c \end{cases} \tag{1}$$

where R_{min} is the minimal value in the fingerprint database, and R_{max} is the maximum value on the contrary. The smaller the normalized value is, the stronger the signal strength.

B. OBJECTIVE AND SKETCHES OF CONDITIONAL GAN

The objective function of a conditional GAN is expressed as follows.

$$L(G, D) = E_{x,y}\left[\log D(x, y)\right] + E_{x,z}\left[\log\left(1 - D(x, G(x, z))\right)\right] + \lambda L_p(G) \tag{2}$$

TABLE 1. Variables and instructions.

Variables	Instructions
$A = \{AP_1, AP_2, \ldots, AP_M\}$	a set of APs, its total number is M
$B = \{RP_1, RP_2, \ldots, RP_N\}$	a set of RPs, its total number is N
$C_i = (x_i, y_i, z_i)$	the cartesian coordinate of RP_i
$R_{C_i}^{k,j}$	the RSS value heard from the kth AP at the jth time point in the ith RP. If the sensor can't hear from the kth AP, it's set as a large constant c (e.g. 255)
$R_{C_i}^{j} = \left[R_{C_i}^{1,j}, R_{C_i}^{2,j}, \ldots, R_{C_i}^{M,j}\right]$	the fingerprint vector of all APs in the ith RP at the jth time point
$R_{C_i} = \begin{bmatrix} R_{C_i}^{1,1} & R_{C_i}^{2,1} & \cdots & R_{C_i}^{M,1} \\ R_{C_i}^{1,2} & R_{C_i}^{2,2} & \cdots & R_{C_i}^{M,2} \\ \vdots & & \ddots & \vdots \\ R_{C_i}^{1,t} & R_{C_i}^{2,t} & \cdots & R_{C_i}^{M,t} \end{bmatrix}$	the fingerprint database of the ith RP, and t is the measurement count
$R = \left[R_{C_1}^T, R_{C_2}^T, \ldots, R_{C_N}^T\right]^T$	the fingerprint database in the offline phase
$s_{C_i}^{k,j} = \begin{cases} 1, & R_{C_i}^{k,j} = c \\ \mu_{C_i}^k, & R_{C_i}^{k,j} < c \end{cases}$	the initial value corresponding to $R_{C_i}^{k,j}$ in a sketch, and $\mu_{C_i}^k$ is different with sketches

where x is remarked as a condition that is the observed data or sketch, and is the input of the generator G and the discriminator D simultaneously; y is the real sample data, and is the input of the D; z is the random noise vector, and is the input of the G; λ is a learning argument. In the network, G tries to minimize this objective against D that tries to maximize it, such as $G^* = arg\ min_G max_D L(G, D)$, and $L_p(G)$ is L1 gradient penalty for G and defined as:

$$L_p(G) = E_{x,y,z}\left[\|(y - G(x, z)) \cdot (G(x, z) - y)\|_1\right] \quad (3)$$

The penalty is to narrow the gap between the real and the fake, e.g., the real is very large but the fake is very small, or the real is negative but the fake is positive. Typically, the penalty of the second case is larger than the first.

To train GAN rapidly and stably, two sketches described the rough outline of the fingerprint database are proposed as the network's conditions. Although the simplest sketch is the real data, it would lead to overfitting and make the network instable.

With real RPs, sketches are the same as the fingerprint database but without real RSS values replaced by $s_{C_i}^{k,j}$, whose value is set to 0, 1, or a mean value. The value 0 means that the real RSS is valid and 1 is on the contrary. Straightforwardly, the mean value can be set equally to the average value of the real data heard from an AP in a RP. If so, the sketch is so perfect as to overfit, and the network loses to learn data fluctuation feature and others. Alternatively, the mean is set to the mean value of the Gaussian Model on the assumption that RSSs heard from an AP in a RP obey Gaussian distribution. In this case, RSSs heard from the same AP in different RPs obey Gaussian Mixture Models (GMMs). With unknown distances between AP and RPs, each Gaussian model's mean can be calculated by the expectation maximization (EM) algorithm [61] shown as Algorithm EM.

Algorithm EM

GMM Definition:

$$P\left(R_{C_i}^k\right) = \sum_{l=1}^{L} \alpha_l \phi\left(R_{C_i}^k \mid \theta_l\right) \quad (4)$$

where $l = 1, 2, \cdots, L$, L is the count of GMMs; $\alpha_l > 0$ and $\sum_{l=1}^{L} \alpha_l = 1$; $\phi\left(R_{C_i}^k \mid \theta_l\right)$ is the lth Gaussian model with unknown argument $\theta_l(\mu_l, \sigma_l^2)$, where μ_l, σ_l^2 are the mean and variance.

Inputs: the RSS fingerprint matrix R, GMMs.

Outputs: arguments of GMMs.

- Step 1: initializing the rough values of α_l, θ_l and L with R.
- Step 2 is the expectation step (E step): calculating the expected value of γ_l^k.

//γ_l^k is defined as the unobserved latent variable represented the distance between the kth AP and ith RP, and initialized with 0 or 1 (1: the observed data $R_{C_i}^k$ belongs to the lth model, 0: the others).

$$\bar{\gamma}_l^k = E\left(\bar{\gamma}_l^k \mid R_{C_i}^k, \theta_l\right) = \frac{\alpha_l \phi\left(R_{C_i}^k \mid \theta_l\right)}{\sum_{l=1}^{L} \alpha_l \phi\left(R_{C_i}^k \mid \theta_l\right)} \quad (5)$$

- Step 3 is the maximization step (M step): calculating the parameters to maximize the maximum likelihood of the GMM.

$$\begin{cases} \bar{\mu}_l = \sum_{i=1}^{N} \bar{\gamma}_l^k . R_{C_i}^k \Big/ \sum_{i=1}^{N} \bar{\gamma}_l^k \\ \bar{\sigma}_l^2 = \sum_{i=1}^{N} \bar{\gamma}_l^k . \left(R_{C_i}^k - \bar{\mu}_l\right)^2 \Big/ \sum_{i=1}^{N} \bar{\gamma}_l^k \\ \bar{\alpha}_l = \sum_{i=1}^{N} \bar{\gamma}_l^k \Big/ N \end{cases} \quad (6)$$

- Step 4: iterating step 2 and step 3 until convergence.

Under the condition of virtual RPs without the real or fake data, the value $s_{C_i}^{k,j}$ is set to 0 directly when a virtual RP's two neighbor RPs are both heard from an AP, and set to 1 otherwise. After generating, it can be set to 0,1, or a mean value estimated by Algorithm EM with the fake data.

All abovementioned sketches are defined as the complete sketches since their structures are the same as the fingerprint databases. Hence, the sketch values not 1 are randomly dropped with a special percent (dropout rate) and set to 1 to prevent overfitting further. If all sketch values are dropped, the sketch is defined as non-sketch, and it's the same as no outline condition. Simply, the sketch with value 0 or 1 is defined as 0-1 Sketch, and the other with the mean value or 1 is defined as Gaussian Sketch.

With a virtual RP, the number of the value 0 in 0-1 Sketch or the mean value in Gaussian Sketch is almost equal to the number of APs heard in the real scenes. Since, normally, the distance between its two neighbor RPs is much smaller than AP's communication distance, and all three RPs are in

the similar scenario at the same time. Hence, all complete sketches are trimmed with the uniform dropout rate.

C. DATA AUGMENTER

In the training phase, the remainder is to design a training mode with a certain network and its inputs, objective function, conditions, etc. In this section, two algorithms with different training modes are proposed and defined as Algorithm 1 and Algorithm 2 separately. Phenomenally, Algorithm 1 is trained with the real data only once, however, the other is trained iteratively with both the real and the fake data. Their structures are shown in Fig. 1, and their steps and corresponding illustrations are defined.

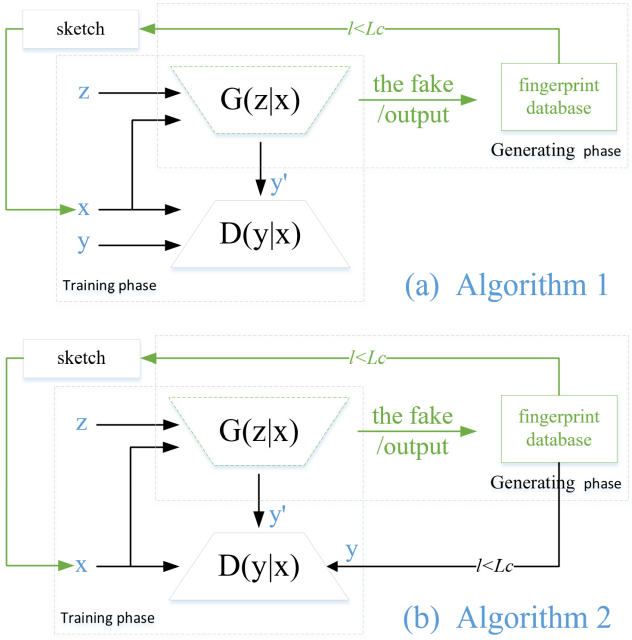

FIGURE 1. Structures of algorithm 1 and algorithm 2.

Algorithm 1 Progressive RSS Data Augmenter

- Step 1: initializing variables in Table 1, a sketch and the objective level L_c.

$//L_c = \lceil avr\,(d_{0i}) / avr\,(d_{L_{ci}}) \rceil avr\,(d_{L_{ci}})$ //$avr\,(d_{0i})$ is the mean distance of neighbor RPs in the initial level 0; $avr\,(d_{L_{ci}})$ is the mean distance in the target level L_c.

- Step 2: training the conditional GAN.
- Step 3: calculating coordinates of virtual RPs at the lth level.

//any virtual RP is the center or the inflexion of neighbor RPs.

- Step 4: generating the fake RSS by the trained generator G with the sketch.

updating the sketch with the generating data; //since RSS and its corresponding information of RPs including the real and fake are different in each level.
setting $l = l + 1$.

- Step 5: iterating step 3 and step 4 until $l = L_c$.

Algorithm 2 Cyclically Progressive RSS Data Augmenter

- Step 1: initializing variables in Table 1, a sketch and the objective level L_c.
- Step 2: training the conditional GAN.
- Step 3: calculating coordinates of virtual RPs at the lth level.
- Step 4: generating the fake RSS by the trained generator G with the sketch.

mixing the new fake RSS with the existing data, and updating variables in Table 1.
updating the sketch with the generating data.
setting $l = l + 1$.

- Step 5: iterating from step 2 to step 4 until $l = L_c$.

III. DATA AUGMENTER QUANTITATIVE EVALUATION MEASURES

In this section, several quantitative measures are proposed to evaluate performances of these algorithms with varying sketches.

A. PROPORTION HEARD SIMULTANEOUSLY (HP)

It describes the fake data quality in a low resolution. In the training phase, a fake RSS should be smaller than the constant c when its corresponding real data heard from the kth AP is valid in the same RP.

$$HP = \frac{\sum_{i=1}^{N_B} \frac{n_i}{N_i}}{N_B} \tag{7}$$

where N_B is the batch size of the real; n_i is the count that RSS values are smaller than the constant c simultaneously in the fake set and the real set; N_i is the count where the real values smaller than the constant c. HP is a meaningful value when the network is stable, because it would be larger than one at the beginning. To avoid this invalid case, its maximum value is set to 1. As an artificial index, it represents a penalty of the generator's loss function in the opposite sign case.

B. RATIONAL FLUCTUATION PROPORTION (RFP)

RSS heard from an AP in a fixed RP obeys the Gaussian distribution. This index indicates that the fake should obey the same Gaussian distribution as the real in the same scene. It is also used in G's loss function as a penalty to generate valid values.

$$RF = \frac{\sum_{i=1}^{N_B} \frac{n_i}{N_i}}{N_B} \tag{8}$$

where n_i is the count of the fake while it is between $\mu_l^k - \sigma_l^k$ and $\mu_l^k + \sigma_l^k$, and μ_l^k and σ_l^k are the mean and variance of the Gaussian distribution, and calculated by the Algorithm EM with the kth AP's RSSs in a RP;N_i is the count of the real

valid values of the kth AP which are smaller than the constant c in the same RP.

C. DIVERSITY SCORE (DS)

As usually, very small RSS is invalid and it can be considered as the constant c. This index represents the case that the real is very small (e.g. -90dB) but the fake is constant c, and the case that the real is constant c but the fake is very small. It indicates the network's generalization ability.

$$DS = \frac{\sum_{i=1}^{N_B} n_i}{N_B} \tag{9}$$

where n_i is the count of diverse data in both cases above.

D. INCEPTION SCORE OF RSS (RIS)

In the image area, Inception Score [62] is perhaps the most widely adopted score for GAN evaluation. It uses a pre-trained neural network (the Inception Net [63] trained on the ImageNet [64]) to capture the desirable properties of generated samples: highly classifiable and diverse with respect to class labels. In the WiFi-based localization area, the score uses Bayesian classifier [65] instead of the Inception Net.

It measures the average KL divergence between the conditional label distribution $p(\boldsymbol{c} \mid \boldsymbol{y}')$ of samples and the marginal distribution $p(\boldsymbol{c})$ obtained from all the samples. It favors low entropy of $p(\boldsymbol{c} \mid \boldsymbol{y}')$ (better sample quality) but a large entropy of $p(\boldsymbol{c})$ (high diversity).

$$exp(E_x[KL(p(\boldsymbol{c} \mid \boldsymbol{y}')||p(\boldsymbol{c}))]) = exp(H(\boldsymbol{c}) - E_x[H(\boldsymbol{c} \mid \boldsymbol{y}')]) \tag{10}$$

where $H(\boldsymbol{c})$ represents entropy of variable $\boldsymbol{c}$; and $p(\boldsymbol{c})$ is the marginal distribution:

$$p(\boldsymbol{c}) \approx \frac{1}{N} \sum_{n=1}^{N} p\left(\boldsymbol{c} \mid \boldsymbol{y}_{\boldsymbol{n}}' = G(\boldsymbol{z}_{\boldsymbol{n}})\right) \tag{11}$$

The conditional label distribution $p\left(\boldsymbol{c} \mid \boldsymbol{y}'\right)$ can be calculated by Bayesian:

$$p\left(\boldsymbol{c} \mid \boldsymbol{y}'\right) = \frac{p\left(\boldsymbol{y}' \mid c_i\right) p\left(c_i\right)}{\sum_{i=1}^{N} p\left(\boldsymbol{y}' \mid c_i\right) p\left(c_i\right)} \tag{12}$$

where $\mathbf{y}'$ is the fake RSS vector; $\boldsymbol{c}$ is the localization label vector, and c_i is the coordinate of ith RP; $p(c_i)$ obeys uniform distribution $(1, N)$, N is the count of RPs.

Supposing that RSSs heard from APs in one same RP are independent, $p\left(\boldsymbol{y}' \mid c_i\right)$ can be calculated by:

$$p\left(\boldsymbol{y}' \mid c_i\right) = p\left(y_1' \mid c_i\right) \times p\left(y_2' \mid c_i\right) \times \cdots \times p\left(y_m' \mid c_i\right) \tag{13}$$

where m is the count of APs heard by a sensor in fixed RP and m is smaller than or equal to M;$p\left(y_i' \mid c_i\right)$ obeys Gaussian distribution $(\mu_{y_i'}, \sigma_{y_i'})$ calculated by the Algorithm EM with data samples.

E. SPARSE PROPORTION (SP)

Under the conditions of the same fingerprinting matching method and the given accuracy metric (i.e. 1 meter), it needs N RPs without a data augmenter and n RPs in this paper. Hence, SP is defined as $1 - n/N$. By fixed conditions, the larger SP is, the better. It indicates data augmenters' effects directly and validly.

IV. EXPERIMENTS AND RESULTS

In this section, we evaluate performances of the two algorithms with different sketches in two aspects: quantitative evaluation measures and localization accuracy. Meanwhile, we analyze the influences of sketches' dropout rates on the algorithms. The results are valuable and help to select an algorithm with a sketch to generate more valid RSS data in a specific application scene.

A. EXPERIMENTAL ENVIRONMENT

Indoor experiments were conducted in our working room with a size of approximately 21 m by 13 m, where WiFi signal is available through installed APs (total 10 in test). There are many obstacles (e.g. desks, chairs, persons, cabinets, etc.) and walls, forming the complex radio propagation environment, as shown in Fig. 2. 120 RPs were collected and the distances between two adjacent RP fluctuated from 0.8 m-3.2 m due to the specific distribution of obstacles. Three testers equipped with different Android phones, including a Samsung Galaxy S9, a Realme X and a Huawei Mate20, participated in the data collection simultaneously. In the offline phase, the dataset was collected over two days, while each tester stayed at one RP in five minutes. In the online phase, each tester walked at one meter per second repeatedly to collect test data.

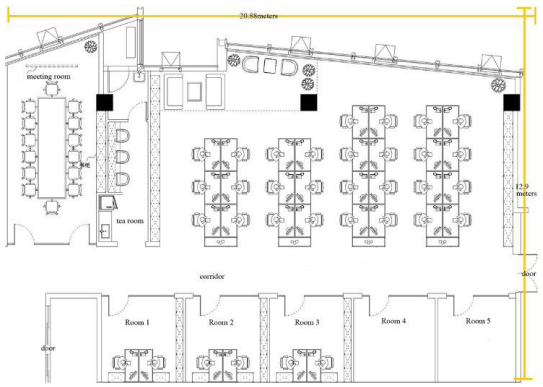

FIGURE 2. The indoor environment.

B. NETWORK ARCHITECTURE

To analyze efforts of the two algorithms, six networks are defined in Table 2, and they have the same architectures shown in Table 3 and Table 4. Architectures of G and D are designed by the empirical evaluation [66] and experiment effects. In Table 3 and Table 4, kernel size is described in format [height (h), width (w), stride], input shape is h × w

TABLE 2. Network defines.

Network	Descriptions
GAN	Algorithm 1 based on GAN
Re-GAN	Algorithm 2 based on GAN
CGAN	Algorithm 1 based on CGAN with 0-1 sketch
Re-CGAN	Algorithm 2 based on CGAN with 0-1 sketch
GGAN	Algorithm 1 based on CGAN with Gaussian sketch
Re-GGAN	Algorithm 2 based on CGAN with Gaussian sketch

TABLE 3. Generator architecture.

Layer	Kernel	Output Shape
z	-	100
Linear, BN, ReLU	-	$h \times w/16 \times 512$
Deconv, BN, ReLU	[5, 5, 2]	$h \times w/8 \times 256$
Deconv, BN, ReLU	[5, 5, 2]	$h \times w/4 \times 128$
Deconv, BN, ReLU	[5, 5, 2]	$h \times w/2 \times 64$
Deconv, Tanh	[5, 5, 2]	$h \times w \times 1$

TABLE 4. Discriminator architecture.

Layer	Kernel	Output Shape
Conv, lReLU	[1, 2, 2]	$h \times w \times 64$
Conv, BN, lReLU	[1, 2, 2]	$h \times w/2 \times 128$
Conv, BN, lReLU	[1, 2, 2]	$h \times w/4 \times 256$
Conv, BN, lReLU	[1, 2, 2]	$h \times w/8 \times 512$
Linear	-	1

and output shape is h × w × channel. Other arguments of the architectures are set as follows: Batch Size=64, Training Epoch=100, Learning Rate=0.0002 and optimizer is Adam.

The training PC is equipped with Intel(R) Xeon(R) CPU E5-1620 v4 CPU, 32GB memory, a Nvidia TITAN Xp display card, 500GB SSD and 2TB disk.

C. INFLUENCES OF SKETCHES ON GENERATING RESULTS

In this part, the key point is to analyze influences of sketches with different dropout rates on Algorithm 1. We train GAN, CGAN and GGAN with real data collected in all 120 RPs. Here, we do not analyze the influences on Algorithm 2, because: a) the real data is enough to train networks, b) it's better to illustrate influences of varying parameters on generators directly and clearly with only real data, c) Algorithm 2 has a variable data volume due to the fake, so it's hard to illuminate results, and d) we analyzed the localization accuracies after proper parameters were selected in the next part, and they can illustrate the two algorithms' performances directly.

We changed the dropout rate of sketches from ten percent to 1. It means that a certain percent of APs aren't heard in sketches but heard in reality. Meanwhile, considering the room size, receiver can hear from almost all APs anywhere (either the real or the virtual RP). So, the dropout rate of sketches is set uniformly in the real and fake cases.

To illustrate directly, we selected the reserving rate (100 - dropout rate) in Fig. 3. We provided the source code and common dataset on the website https://github.com/shutaozh/data_augmenter_with_CGAN. Results are shown in Fig. 3.

Some conclusions based on Fig. 3 are shown as follows.

1) The quality of data generated by either CGAN or GGAN is better than GAN due to the conditions from artificial experiences.
2) All three networks' diversities are poor, due to the generator's penalty is inclined to the data quality.
3) HP, RFP and RIS are good once the dropout rate is smaller than 0.6. When the dropout rate is one or close to 1, sketches are hard to describe the outline of the fingerprint database. In this case, either CGAN or GGAN is nearly equal to GAN.
4) CGAN is nearly equal to GGAN since features of the real data are learned by the adversarial networks automatically, and element values of sketches have almost no effects on qualities of the generating data.

Meanwhile, the convergence rate of GAN is slower than the others, and GGAN is trained fastest. And, GAN diverged many times in a limited epoch.

D. LOCALIZATION ACCURACY AND SP ANALYSIS

We selected KNN, which is seriously relied on the RP's count, to analyze localization accuracies of the two algorithms. we varied the RP count from ten percent to hundred percent of all 120 RPs, by the way of scaling up the distance between adjacent RPs.

TABLE 5. Localization accuracy by varying RPs.

The percent of RPs	10	20	30	40	50	60	70	80	90	100
Real data	8.757	8.532	7.358	4.749	3.942	3.079	2.745	1.855	0.783	1.235
GAN	8.864	8.352	6.945	5.137	4.589	3.627	3.311	1.574	0.973	0.841
CGAN	8.918	8.246	4.825	3.795	3.028	2.308	1.354	0.776	0.778	0.778
GGAN	9.103	8.174	5.473	3.987	2.831	2.174	1.135	0.724	0.738	0.678
Re-CGAN	7.785	7.832	7.085	3.514	2.331	1.371	1.803	1.793	1.779	1.722
Re-GGAN	7.794	7.652	6.843	3.744	2.154	1.756	2.031	1.645	2.013	2.115

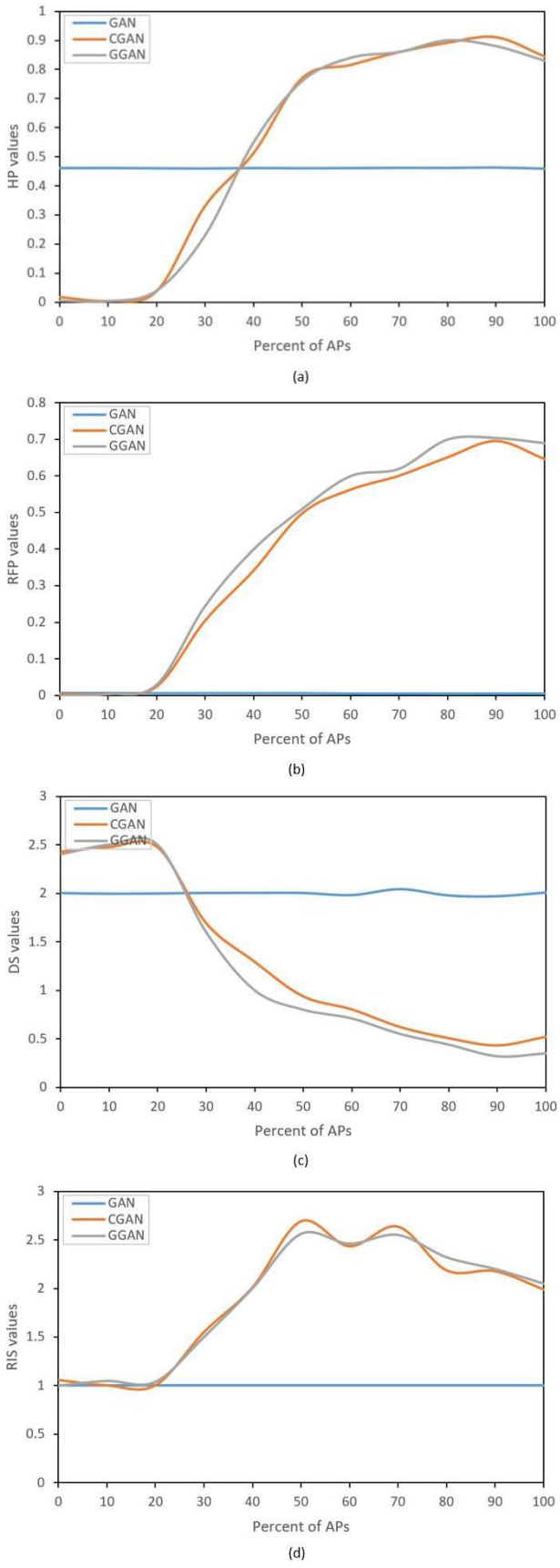

FIGURE 3. Indicators of the three networks by varying APs. (a) HP index. (b) RFP index. (c) DS index. (d) RIS index.

Based on the above part, we set dropout rate as 0.4, and set k=3 and Euclidean distance of KNN. Results are shown in Table 5.

Conclusions are shown as follows.

1) Localization accuracies of any data augmenter except GAN are better than no augmenter when the percent is larger than 20 and smaller than 80. Reasons are: a) all networks are good as long as the training data is enough, b) the fake data is valid except GAN, and c) accuracies are depended on KNN after RPs are enough.
2) Algorithm 1 (CGAN or GGAN) has poorer performance than Algorithm 2 (Re-CGAN or Re-GGAN) as the percent is smaller than 70. The reasons are that the real and the fake data enrich the fingerprint database for cyclically training in Algorithm 2, and the networks of Algorithm 2 have strong antijamming capability to the fake.
3) Algorithm 1 is better than Algorithm 2 when the percent is larger than 60. The reasons are: a) the data is enough to train all networks, and b) it has a little influence of the inaccurate fake data on generator's parameters in Algorithm 2.
4) Algorithm 1 is robust and can improve the localization accuracy after the percent is larger than 80. However, the improvement is limited due to KNN.
5) Fixed localization accuracy index, SP can be inferred by Table 4, and SP of Algorithm 1 is larger than SP of Algorithm 2 when the accuracy index is high and vice versa.

During the experiments, Algorithm 2 is much slower than Algorithm 1 because of training generative adversarial networks repetitively. Typically, augmenter based on Re-GGAN is slowest than others due to the Gaussian sketch. Though Re-GAN was defined, the results are not shown here due to the poor performance of the fake data by GAN.

V. CONCLUSION

To establish the WiFi-based fingerprint database under the condition of sparse RPs, a novel data augmenter based on the conditional adversarial network is proposed. To illustrate its effects, we proposed two algorithms with different sketches, and defined five quantitative evaluation metrics based on the artificial experiences and the data features. Experiments demonstrate:

1) The data augmenters trained with sketches can generate valid fake data to construct fingerprint database with sparse RPs.

2) The fake data is beneficial to improve the localization accuracy;

3) In the comprehensive point of view, Algorithm 1 with the 0-1 sketch is more effective and stable than others;

4) We also found that all of adversarial networks without gradient penalty were hardly convergent in a limited epoch. The quantitative evaluation metrics are significant to improve the network quality and the data.

In the future, a new localization mapping approach should be studied to improve accuracy with the fake data. Meanwhile, combining our algorithm with some other fitting or interpolation methods to construct fingerprint database with extremely little RPs.

REFERENCES

[1] (May 2016). *Galileo*. [Online]. Available: http://www.gsa.europa.eu/galileo/why-galileo
[2] (May 2016). *Beidou*. [Online]. Available: http://en.beidou.gov.cn/
[3] A. Bandyopadhyay, D. Hakim, B. Funk, E. Kohn, C. Teolis, and G. Blankenship, "System and method for locating, tracking, and/or monitoring the status of personnel and/or assets both indoors and outdoors," U.S. Patent 8 712 686, Apr. 2014.
[4] R. Giuliano, F. Mazzenga, M. Petracca, and M. Vari, "Indoor localization system for first responders in emergency scenario," in *Proc. 9th Int. Wireless Commun. Mobile Comput. Conf. (IWCMC)*, Jul. 2013, pp. 1821–1826.
[5] K. Wang, A. Nirmalathas, C. Lim, K. Alameh, H. Li, and E. Skafidas, "Indoor infrared optical wireless localization system with background light power estimation capability," *Opt. Express*, vol. 25, no. 19, pp. 22923–22931, Sep. 2017.
[6] H. Ma and K. Wang, "Fusion of RSS and phase shift using the Kalman filter for RFID tracking," *IEEE Sensors J.*, vol. 17, no. 11, pp. 3551–3558, Jun. 2017.
[7] Y. Zhao, K. Liu, Y. Ma, Z. Gao, Y. Zang, and J. Teng, "Similarity analysis based indoor localization algorithm with backscatter information of passive UHF RFID tags," *IEEE Sensors J.*, vol. 17, no. 1, pp. 185–193, Jan. 2017.
[8] J. N. Moutinho, R. E. Araújo, and D. Freitas, "Indoor localization with audible sound—Towards practical implementation," *Pervasive Mobile Comput.*, vol. 29, pp. 1–16, Jul. 2016.
[9] W. Elloumi, A. Latoui, R. Canals, A. Chetouani, and S. Treuillet, "Indoor pedestrian localization with a smartphone: A comparison of inertial and vision-based methods," *IEEE Sensors J.*, vol. 16, no. 13, pp. 5376–5388, Jul. 2016.
[10] M. Castillo-Cara, J. Lovón-Melgarejo, G. Bravo-Rocca, L. Orozco-Barbosa, and I. García-Varea, "An empirical study of the transmission power setting for Bluetooth-based indoor localization mechanisms," *Sensors*, vol. 17, no. 6, p. 1318, Jun. 2017.
[11] Y. Wang and L. Shao, "Understanding occupancy pattern and improving building energy efficiency through Wi-Fi based indoor positioning," *Building Environ.*, vol. 114, pp. 106–117, Mar. 2017.
[12] F. Zafari, A. Gkelias, and K. Leung, "A survey of indoor localization systems and technologies," Mar. 2018, *arXiv:1709.01015*. [Online]. Available: https://arxiv.org/abs/1709.01015
[13] D. Lymberopoulos and J. Liu, "The microsoft indoor localization competition: Experiences and lessons learned," *IEEE Signal Process. Mag.*, vol. 34, no. 5, pp. 125–140, Sep. 2017.
[14] W. He, P.-H. Ho, and J. Tapolcai, "Beacon deployment for unambiguous positioning," *IEEE Internet Things J.*, vol. 4, no. 5, pp. 1370–1379, Oct. 2017.
[15] K. Lin, M. Chen, J. Deng, M. M. Hassan, and G. Fortino, "Enhanced fingerprinting and trajectory prediction for IoT localization in smart buildings," *IEEE Trans. Automat. Sci. Eng.*, vol. 13, no. 3, pp. 1294–1307, Jul. 2016.
[16] X. Guo, L. Li, N. Ansari, and B. Liao, "Knowledge aided adaptive localization via global fusion profile," *IEEE Internet Things J.*, vol. 5, no. 2, pp. 1081–1089, Apr. 2018.
[17] X. Guo, L. Li, N. Ansari, and B. Liao, "Accurate WiFi localization by fusing a group of fingerprints via a global fusion profile," *IEEE Trans. Veh. Technol.*, vol. 67, no. 8, pp. 7314–7325, Aug. 2018.
[18] A. Khalajmehrabadi, N. Gatsis, D. J. Pack, and D. Akopian, "A joint indoor WLAN localization and outlier detection scheme using LASSO and elastic-net optimization techniques," *IEEE Trans. Mobile Comput.*, vol. 16, no. 8, pp. 2079–2092, Aug. 2017.
[19] C. Xu, B. Firner, Y. Zhang, and R. E. Howard, "The case for efficient and robust RF-based device-free localization," *IEEE Trans. Mobile Comput.*, vol. 15, no. 9, pp. 2362–2375, Sep. 2016.
[20] P. Davidson and R. Piche, "A survey of selected indoor positioning methods for smartphones," *IEEE Commun. Surveys Tutr.*, vol. 19, no. 2, pp. 1347–1370, 2nd Quart., 2017.
[21] M. Youssef and A. Agrawala, "The Horus WLAN location determination system," in *Proc. 3rd Int. Conf. Mobile Syst., Appl., Services (MobiSys)*, Seattle, WA, USA, Jun. 2005, pp. 205–218.
[22] Y. Zhuang, J. Yang, Y. Li, L. Qi, and N. El-Sheimy, "Smartphone-based indoor localization with Bluetooth low energy beacons," *Sensors*, vol. 16, no. 5, p. 596, Apr. 2016.
[23] M. Oussalah, M. Alakhras, and M. I. Hussein, "Multivariable fuzzy inference system for fingerprinting indoor localization," *Fuzzy Sets Syst.*, vol. 269, pp. 65–89, Jun. 2015.
[24] A. Rozyyev, H. Hasbullah, and F. Subhan, "Combined K-nearest neighbors and fuzzy logic indoor localization technique for wireless sensor network," *Res. J. Inf. Technol.*, vol. 4, no. 4, pp. 155–165, Apr. 2012.
[25] C. Figuera, J. L. Rojo-Álvarez, M. Wilby, I. Mora-Jiménez, and A. J. Caamaño, "Advanced support vector machines for 802.11 indoor location," *Signal Process.*, vol. 92, no. 9, pp. 2126–2136, Sep. 2012.
[26] J. Hong and T. Ohtsuki, "Signal eigenvector-based device-free passive localization using array sensor," *IEEE Trans. Veh. Technol.*, vol. 64, no. 4, pp. 1354–1363, Apr. 2015.
[27] J. Zou, X. Guo, L. Li, S. Zhu, and X. Feng, "Deep regression model for received signal strength based WiFi localization," in *Proc. IEEE 23rd Int. Conf. Digit. Signal Process. (DSP)*, Nov. 2018, pp. 1–4.
[28] Y. Li, Z. Gao, Z. He, Y. Zhuang, A. Radi, R. Chen, and N. El-Sheimy, "Wireless fingerprinting uncertainty prediction based on machine learning," *Sensors*, vol. 19, no. 2, p. 324, Jan. 2019.
[29] L. Zhao, H. Huang, X. Li, S. Ding, H. Zhao, and Z. Han, "An accurate and robust approach of device-free localization with convolutional autoencoder," *IEEE Internet Things J.*, vol. 6, no. 3, pp. 5825–5840, Jun. 2019.
[30] K.-W. Chiang, A. Noureldin, and N. El-Sheimy, "A new weight updating method for INS/GPS integration architectures based on neural networks," *Meas. Sci. Technol.*, vol. 15, no. 10, pp. 2053–2061, Jun. 2004.
[31] Z. Turgut, S. Üstebay, G. Z. G. Aydin, and A. Sertbaş, "Deep learning in indoor localization using WiFi," in *Proc. Int. Telecommun. Conf.*, Istanbu, Turkey, Dec. 2018, pp. 101–110.
[32] X. Wang, L. Gao, S. Mao, and S. Pandey, "CSI-based fingerprinting for indoor localization: A deep learning approach," *IEEE Trans. Veh. Technol.*, vol. 66, no. 1, pp. 763–776, Jan. 2017.
[33] X. Wang, L. Gao, and S. Mao, "CSI phase fingerprinting for indoor localization with a deep learning approach," *IEEE Internet Things J.*, vol. 3, no. 6, pp. 1113–1123, Dec. 2016.
[34] Z. E. Khatab, A. Hajihoseini, and S. A. Ghorashi, "A fingerprint method for indoor localization using autoencoder based deep extreme learning machine," *IEEE Sensors Lett.*, vol. 2, no. 1, Mar. 2018, Art. no. 6000204.
[35] H. Chen, Y. Zhang, W. Li, X. Tao, and P. Zhang, "ConFi: Convolutional neural networks based indoor Wi-Fi localization using channel state information," *IEEE Access*, vol. 5, pp. 18066–18074, 2017.
[36] X. Wang, X. Wang, and S. Mao, "CiFi: Deep convolutional neural networks for indoor localization with 5GHz Wi-Fi," in *Proc. ICC*, Paris, France, May 2017, pp. 1–6.
[37] W. Wang, X. Wang, and S. Mao, "Deep convolutional neural networks for indoor localization with CSI images," *IEEE Trans. Netw. Sci. Eng.*, to be published. [Online]. Available: https://ieeexplore.ieee.org/ document/8468057
[38] M. Nowicki and J. Wietrzykowski, "Low-effort place recognition with WiFi fingerprints using deep learning," in *Proc. Integr. Comput.-Aided Eng.*, 2017, pp. 575–584.
[39] K. S. Kim, S. Lee, and K. Huang, "A scalable deep neural network architecture for multi-building and multi-floor indoor localization based on Wi-Fi fingerprinting," *Big Data Anal.*, vol. 3, no. 1, p. 4, Dec. 2018.
[40] W. Zhang, K. Liu, W. Zhang, Y. Zhang, and J. Gu, "Deep Neural Networks for wireless localization in indoor and outdoor environments," *Neurocomputing*, vol. 194, pp. 279–287, Jun. 2016.
[41] G. Aceto, D. Ciuonzo, A. Montieri, and A. Pescapé, "Mobile encrypted traffic classification using deep learning," in *Proc. Netw. Traffic Meas. Anal. Conf. (TMA)*, Jun. 2018, pp. 1–8.
[42] W. Wang, M. Zhu, X. Zeng, X. Ye, and Y. Sheng, "Malware traffic classification using convolutional neural network for representation learning," in *Proc. Int. Conf. Inf. Netw. (ICOIN)*, Jan. 2017, pp. 712–717.
[43] W. Shao, H. Luo, F. Zhao, C. Wang, A. Crivello, and M. Z. Tunio, "DePos: Accurate orientation-free indoor positioning with deep convolutional neural networks," in *Proc. Ubiquitous Positioning, Indoor Navigat. Location-Based Services (UPINLBS)*, Mar. 2018, pp. 1–7.
[44] A. Mittal, S. Tiku, and S. Pasricha, "Adapting convolutional neural networks for indoor localization with smart mobile devices," in *Proc. Great Lakes Symp. (GLSVLSI)*, Chicago, IL, USA, 2018, pp. 117–122.

[45] J. Liu, L. Wang, J. Fang, L. Guo, B. Lu, and L. Shu, "Multi-target intense human motion analysis and detection using channel state information," *Sensors*, vol. 18, no. 10, p. 3379, Oct. 2018.
[46] A. Khalajmehrabadi, N. Gatsis, and D. Akopian, "Indoor WLAN localization using group sparsity optimization technique," in *Proc. IEEE/ION Position, Location Navigat. Symp. (PLANS)*, Apr. 2016, pp. 584–588.
[47] C. Feng, W. S. A. Au, S. Valaee, and Z. Tan, "Received-signal-strength-based indoor positioning using compressive sensing," *IEEE Trans. Mobile Comput.*, vol. 11, no. 12, pp. 1983–1993, Dec. 2012.
[48] A. Tabibiazar and O. Basir, "Compressive sensing indoor localization," in *Proc. IEEE Int. Conf. Syst., Man, Cybern.*, Oct. 2011, pp. 1986–1991.
[49] R. Anshul, K. K. Chintalapudi, V. N. Padmanabhan, and R. Sen, "Zee: Zero-effort crowdsourcing for indoor localization," in *Proc. 18th Annu. Int. Conf. Mobile Comput. Netw.*, Istanbul, Turkey, 2012, pp. 293–304.
[50] Y. Shu, Y. Huang, J. Zhang, P. Coue, P. Cheng, J. Chen, and K. G. Shin, "Gradient-based fingerprinting for indoor localization and tracking," *IEEE Trans. Ind. Electron.*, vol. 63, no. 4, pp. 2424–2433, Apr. 2016.
[51] H. Zou, M. Jin, H. Jiang, L. Xie, and C. J. Spanos, "WinIPS: WiFi-based non-intrusive indoor positioning system with online radio map construction and adaptation," *IEEE Trans. Wireless Commun.*, vol. 16, no. 12, pp. 8118–8130, Dec. 2017.
[52] Q. Li, W. Li, W. Sun, J. Li, and Z. Liu, "Fingerprint and assistant nodes based Wi-Fi localization in complex indoor environment," *IEEE Access*, vol. 4, pp. 2993–3004, 2016.
[53] J. Qin, S. Sun, Q. Deng, L. Liu, and Y. Tian, "Indoor trajectory tracking scheme based on delaunay triangulation and heuristic information in wireless sensor networks," *Sensors*, vol. 17, no. 6, p. 1275, Jun. 2017.
[54] Y. Wang, H. Fan, R. Chen, H. Li, L. Wang, K. Zhao, and W. Du, "Positioning locality using cognitive directions based on indoor landmark reference system," *Sensors*, vol. 18, no. 4, p. 1049, Apr. 2018.
[55] C. He, S. Guo, Y. Wu, and Y. Yang, "A novel radio map construction method to reduce collection effort for indoor localization," *Measurement*, vol. 94, pp. 423–431, Dec. 2016.
[56] R. K. Mahapatra and N. S. V. Shet, "Localization based on RSSI exploiting Gaussian and averaging filter in wireless sensor network," *Arabian J. Sci. Eng.*, vol. 43, no. 8, pp. 4145–4159, 2018.
[57] C. H. Tseng and J.-S. Yen, "Enhanced Gaussian mixture model of RSSI purification for indoor positioning," *J. Syst. Archit.*, vol. 81, pp. 1–6, Nov. 2017.
[58] B. Wang, S. Zhou, L. T. Yang, and Y. Mo, "Indoor positioning via subarea fingerprinting and surface fitting with received signal strength," *Pervas. Mobile Comput.*, vol. 23, pp. 43–58, Oct. 2015.
[59] Y. Ye and B. Wang, "RMapCS: Radio map construction from crowdsourced samples for indoor localization," *IEEE Access*, vol. 6, pp. 24224–24238, 2018.
[60] W. Li, B. Wang, L. T. Yang, and M. Zhou, "RMapTAFA: Radio map construction based on trajectory adjustment and fingerprint amendment," *IEEE Access*, vol. 7, pp. 14488–14500, 2019.
[61] L. Chen, X. Li, J. Wang, Q. Li, and W. Sun, "A localization method with dynamic weight argument based on Gaussian mixed Model," in *Proc. Int. Conf. Control, Autom. Inf. Sci. (ICCAIS)*, Oct. 2015, pp. 297–301.
[62] T. Salimans, I. Goodfellow, W. Zaremba, V. Cheung, A. Radford, and X. Chen, "Improved techniques for training gans," in *Proc. Adv. Neural Inf. Process. Syst. (NIPS)*, Barcelona, Spain, 2016, pp. 2234–2242.
[63] C. Szegedy, V. Vanhoucke, S. Ioffe, J. Shlens, and Z. Wojna, "Rethinking the inception architecture for computer vision," in *Proc. IEEE Conf. Comput. Vis. Pattern Recognit. (CVPR)*, Jun. 2016, pp. 2818–2826.
[64] J. Deng, W. Dong, R. Socher, L.-J. Li, K. Li, and L. Fei-Fei, "ImageNet: A large-scale hierarchical image database," in *Proc. IEEE Conf. Comput. Vis. Pattern Recognit.*, Jun. 2009, pp. 248–255.
[65] A. Coluccia and F. Ricciato, "RSS-based localization via Bayesian ranging and iterative least squares positioning," *IEEE Commun. Lett.*, vol. 18, no. 5, pp. 873–876, May 2014.
[66] K. Kurach, M. Lucic, X. Zhai, M. Michalski, and S. Gelly, "The GAN landscape: Losses, architectures, regularization, and normalization," in *Proc. Int. Conf. Mach. Learn.*, 2018, pp. 1–17. [Online]. Available: https://arxiv.org/abs/1807.04720

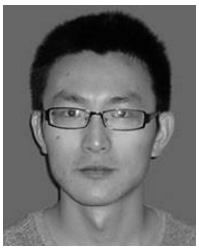

LIANGFENG CHEN received the Ph.D. degree in control theory from the University of Science and Technology, Hefei, China, in 2016. He is currently an Assistant Researcher with the Hefei Institute of Physical Science, Chinese Academy of Sciences, Hefei. His research interests include network security, natural language processing, deep learning, and big data.

SHUTAO ZHANG received the B.S. degree in computer science and technology from Jiangnan University, Wuxi, China, in 2018. He is currently pursuing the M.S. degree in computer applied technology with the University of Science and Technology of China, Hefei, China. His current research interests include artificial intelligence, natural language processing, and big data.

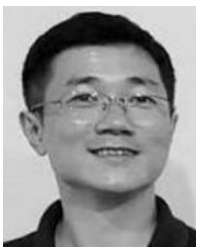

HAIBO TAN is currently a Professor with the Hefei Institute of Physical Science, Chinese Academy Sciences, Hefei, China. His research interests include network security, artificial intelligence, and big data.

BO LV is currently an Assistant Professor with the Hefei Institute of Physical Science, Chinese Academy Sciences, Hefei, China. His research interests include artificial intelligence and big data.